Journal of Ceramic Processing Research. Vol. 24, No. 4, pp. 723~727 (2023)
(Received 1 June 2023, Received in revised form 7 July 2023, Accepted 14 July 2023)
https://doi.org/10.36410/jcpr.2023.24.4.723

J O U R N A L O F
Ceramic Processing Research

Effect of sintering atmosphere on the structure and dielectric properties of BSIT ceramics

Yue Liu[a,#], Kunzhi Luan[a,#], Jiahao Xu[b], Zhen Wang[a], Yike He[a] and Guishan Liu[a,*]
[a]*College of Textile and Materials Engineering, Dalian Polytechnic University, Dalian 116034, China*
[b]*College of Mechanics and Materirals, Hohai University, Nanjing 210024, China*

In this paper, the effects of O_2 and N_2 sintering atmospheres on the physical phase and microstructure of BSIT ceramics were investigated by using In^{3+}-doped BST ceramics as the research object. And then the dielectric properties of the ceramics in the frequency range of 20Hz-300000 Hz were investigated by constructing ceramic capacitors. The results show that the ceramic sintered in N_2 atmosphere has a denser morphology and a higher dielectric constant of 862 compared with the ceramic sintered in O_2 atmosphere, and the dielectric loss is reduced by about 39% in the high frequency stage.

Keywords: In_2Se_3, BST-based ceramics, Sintering atmosphere, Dielectric properties.

Introduction

Ferroelectric materials have a wide range of applications in microwave tuners [1], dynamic random memories (DRAMs) [2], surface acoustic wave devices [3], phase shifters [4] and other devices due to their superior dielectric, piezoelectric, ferroelectric, thermoelectric and optoelectronic properties. Typical ferroelectric materials currently available are $PbZr_xTi_{1-x}O_3$(PZT), (Pb,La)(Zr,Ti)O_3(PLZT), (Pa,La)TiO_3(PLT), $PbTiO_3$, $BaTiO_3$ (BT), barium strontium titanate ((Ba,Sr)TiO_3, BST), $SrBi_2Ta_2O_9$(SBT), etc. Among them, perovskite ABO_3 type BST is a complete solid solution formed by mixing and sintering two materials, barium titanate and strontium titanate, which combines the advantages of both materials and is a ferroelectric material with high dielectric coefficient, strong voltage nonlinearity, low loss and high stability, with the spontaneous polarisation common to ferroelectrics, they are used in a wide range of applications such as capacitors and semiconductor storage [5-7]. However, the high dielectric loss of BST materials leads to the shortened service life and deterioration of the performance of capacitors and other areas, and how to reduce the dielectric loss while maintaining a suitable dielectric constant ($300 < \varepsilon r < 1500$) [8] is a hot topic of current research. The commonly used modification method is doping, such as doping with MgO, La_2O_3, $CaSnO_3$ and other oxides to improve the dielectric properties of BST [9, 10] to improve their dielectric properties in high temperature and high voltage environments. Lin [11] used $CaSnO_3$ to dope modify BST dielectric ceramics. When the doping amount of $CaSnO_3$ was varied from 1.5 wt% to 8 wt%, the dielectric constant of the BST dielectric ceramic samples first decreased, then increased and then decreased, and the dielectric loss first decreased and then increased, and the lowest dielectric loss was 0.069 at a doping concentration concentration of 6 wt%. Jia [12] found that the doping of MgO and La_2O_3 significantly reduced the dielectric constant and losses of BST materials by doping them with MgO and La_2O_3 and testing them using the capacitance method. Also by changing the preparation process such as sintering temperature [13], addition of sintering aids [14], dopant concentration [15], etc. By varying the sintering temperature of the BST ceramics, Jing [16] found that the BST ceramics calcined at 950 °C had the highest densities, a high dielectric constant of 7676 and a dielectric loss of 0.01. Li [17] prepared BST-BZN complex phase ceramics with good dielectric constant temperature stability using 10 wt% Bi_2O_3-$ZnNb_2O_6$ (BZN) as a sintering aid.

The structure and electrical properties of ceramics are also related to the sintering atmosphere, For example, the dielectric constant of BT ceramics sintered in an inert protective atmosphere was significantly improved by Duan [18]. Zhang [19] studied the effect of sintering atmosphere on the properties of SBT ferroelectric ceramics and found that SBT ceramics sintered in an oxygen atmosphere had greater polarization strength and lower coercivity field, which effectively improved the ferroelectric properties of SBT ceramics,and the crystal structure of ceramics prepared under different sintering atmospheres may also be very different [20]. The results of theoretical studies give that the ambient

[#]These authors contributed equally.
*Corresponding author:
Tel : +86-13940966431
E-mail: gshanliu@126.com

atmosphere affects the formation energy of O^{2-} vacancies [21]. Therefore, changing the sintering atmosphere during the preparation of ceramics is expected to change the concentration of oxygen vacancies and cation vacancies in the ceramics, thus changing their electrical properties. In combination with the above, many factors can affect the structure and properties of BST ceramics, but relatively few studies have been reported on the effect of sintering atmosphere on the crystal structure and dielectric properties of BST-based ceramics. In our previous work, we investigated the effect of In_2Se_3 doping on the dielectric properties of BST ceramics, and the results showed that In_2Se_3 doping can reduce the dielectric loss of BST. Therefore, this experiment further investigated the changes in the physical phase structure and surface morphology of the ceramics by sintering with two atmospheres, N_2 and O_2; the effect of sintering atmosphere on the dielectric properties of the ceramics was investigated by preparing ceramic capacitors, in order to obtain a suitable sintering atmosphere and high dielectric and low loss BSIT ceramics.

Experimental Procedure

Preparation of In^{3+}-doped $Ba_xSr_{1-x}TiO_3$(x=0.6) ceramics by sol-gel method:$C_4H_6BaO_4$ and $C_4H_6O_4Sr$ were dissolved in deionized water and labeled as solution A. $C_{16}H_{36}O_4Ti$ and In_2Se_3 were dissolved in ethanol and glacial acetic acid for mixing and labeled as solution B. Solution A was added drop by drop to solution B, stirred to form a more stable purple-black sol, and then left to age for 24 hours and dried at 85 °C for 6 hours in a constant temperature drying oven to form a dry gel. Then calcined at 800 °C under O_2 atmosphere to obtain 2.5% In_2Se_3@BST powder, added 5 wt% PVA and pressed into circular blanks of 10 mm diameter under 10 Mpa pressure. Finally, the BSIT ceramics were produced by sintering in different atmospheres (O_2, N_2) for 4 h at a sintering temperature of 1300 °C and cooling to room temperature with the furnace (noted as sample 1 and sample 2). The electrodes were first made by printing silver paste on both sides of the ceramic sheet at 800 °C to obtain BSIT ceramic capacitor samples.

X-ray diffraction (XRD) characterization by Cu Kα radiation on an X-ray diffractometer (XRD-7000S, Shimadzu, Japan) and morphology and microstructure of BSIT ceramics by field emission scanning electron microscopy (SEM) (JSM-7800F, Oxford, UK); The thickness and diameter of the samples were measured first, and then the capacitance and loss factor of the samples were tested at frequencies from 20 Hz to 30,0000 Hz using an automatic component analyzer (TH2818, Le yi Electronics Co. Ltd. China), and the thickness and diameter of sample 1 and sample 2 were measured separately using vernier calipers first; The relative dielectric coefficients εr and the tangent of the dielectric loss angle tanδ of the samples at the same temperature at different frequencies and at the same frequency at different temperatures are calculated according to Equations (1) and (2):

$$\varepsilon_r = \frac{14.4Ch}{\phi^2} \quad (1)$$

$$\varepsilon\tan\delta = D \quad (2)$$

In formula: h is the thickness of the sample (cm); C is the capacitance of the sample (pF); D is the dielectric loss factor; Φ is the area of the sample; ε air dielectric constant is equal to 1.

Results and Discussion

Ceramic crystal structure and physical phase analysis

Fig. 1 shows the XRD patterns of BSIT ceramics and BST ceramics sintered in N_2 and O_2 calcination atmospheres. As can be seen from the figure, the ceramics obtained by sintering in both atmospheres did not change the composition of the main crystalline phase, the amount of doped In^{3+} did not reach the dissolution saturation of In^{3+} in BST, and thus no second phase was generated, In^{3+} completely enters the perovskite lattice, a=3.965 Å. It suggesting that different sintering atmospheres do not affect the change in the physical phase of BST-based ceramics.However, the intensity of the (110) diffraction peak and other peaks of sample 2 was significantly higher than that of sample 1, indicating that the nitrogen atmosphere was more favorable for BST crystallization.

Surface morphology analysis of ceramics

Fig. 2 and Fig. 3 are the EDS energy spectra of ceramics sintered under two different sintering atmospheres. It can be seen that the elements are uniformly distributed on the surface of the samples, but the distribution of

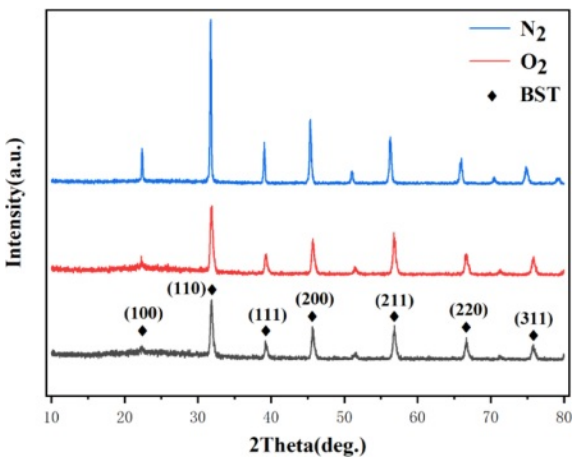

Fig. 1. XRD patterns of BSIT ceramics and BST ceramics sintered after calcination with N_2 and O_2 calcination atmosphere.

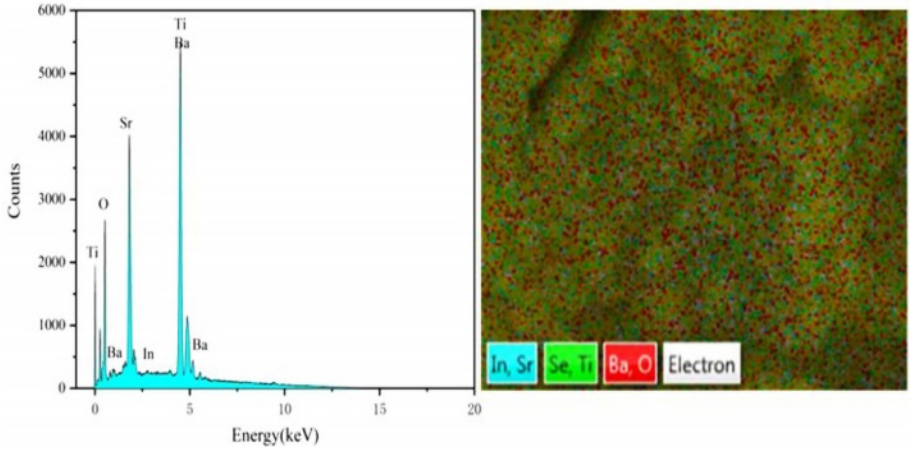

Fig. 2. EDS plot of ceramic samples sintered under O_2 atmosphere.

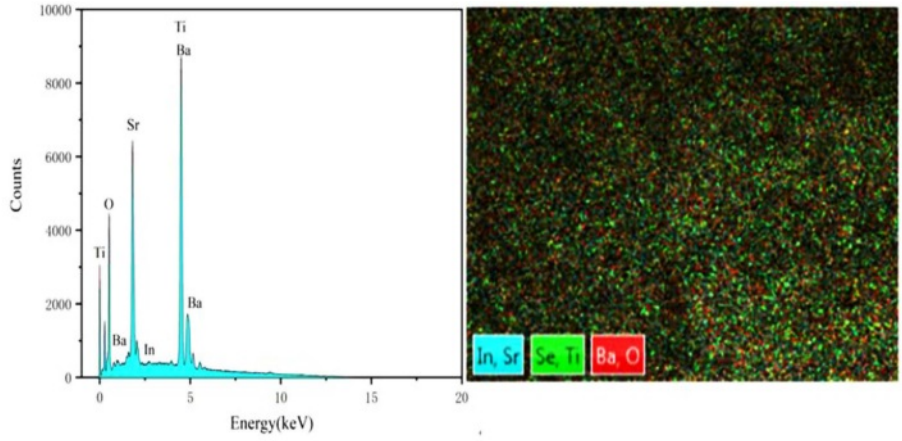

Fig. 3. EDS plot of ceramic samples sintered under N_2 atmosphere.

elements on the surface of sample 2 is more dense, indicating that the particles of sample 2 are closely connected and the surface is more dense; there is no Se element in both samples, and the analysis suggests that it is because the sintering temperature of the ceramics is too high, resulting in the volatilization of Se elements. Fig. 4 shows the SEM images of the ceramics (sample 1) sintered under O_2 and N_2 atmosphere. From the figure, it can be seen that the surface grain morphology of both samples is basically spherical. The microstructure of sample 1 is loose, there are obvious holes, the interface between the grains is blurred, the size is small, the average diameter is 315.16 nm, the porosity is high, while the microstructure of sample 2 is denser, the porosity is low, the grain shape is regular and angular, the grain boundary is clear and flat and

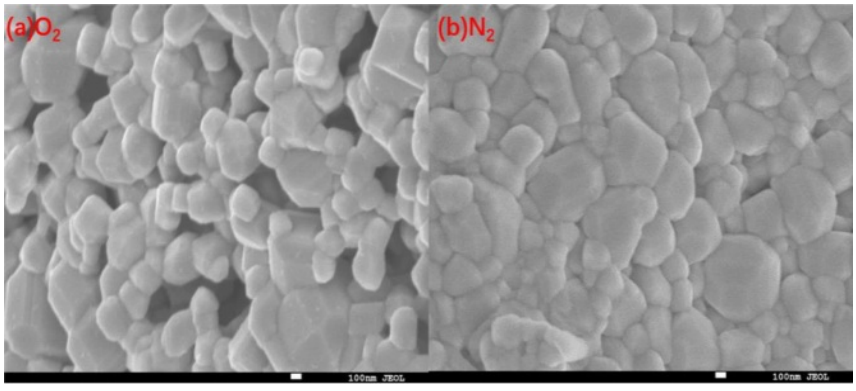

Fig. 4. SEM images of ceramic samples sintered under O_2 (a) and N_2 (b) calcination atmosphere.

continuous distribution, the size shows a trend of increasing, the average diameter is about 569.35 nm. The surface grain size of the two samples is different because the radius and valence of In^{3+} are different from Sr^{2+} and Ba^{2+}. In order to maintain the valence balance, certain vacancies must be generated, and the appearance of vacancies back to cause lattice distortion, lattice distortion to consume a certain amount of energy, but the solute sub-condensation on the grain boundaries with defects do not need to consume energy, so the ions into the BST are easy to deviate in the grain boundaries or near the grain boundaries, resulting in its microscopic surface unevenness. This leads to the unevenness of the microscopic surface. However, due to more oxygen vacancies in the N_2 atmosphere, a reaction (3) occurs:

$$O_o^x \rightarrow V_o + \frac{1}{2}O_2\uparrow + 2e \quad (3)$$

This leads to an increase in vacancy concentration during the sintering process, resulting in an increase in the ion diffusion rate and the formation of BSIT ceramics with a uniform and dense structure. Therefore, the N_2 environment can promote the growth of ceramic grains and enhance the sintering activity of ceramics, thus improving the surface densities of ceramics.

Analysis of the dielectric properties of ceramics

Fig. 5 shows the variation of the dielectric constants of sample 1 and sample 2 between the test frequencies of 20 Hz and 300000 Hz. It can be seen from the figure that the dielectric constants of both samples 1 and 2 largely show a decreasing trend with increasing frequency and the stability increases with frequency, but the dielectric constants of the ceramics in N_2 atmosphere are higher than those in O_2 atmosphere. This is due to the higher oxygen vacancy concentration under N_2 atmosphere, which increases the atomic diffusion rate during the sintering process and enhances the structural homogeneity and densities of the ceramics, which is consistent with the results obtained from SEM maps.

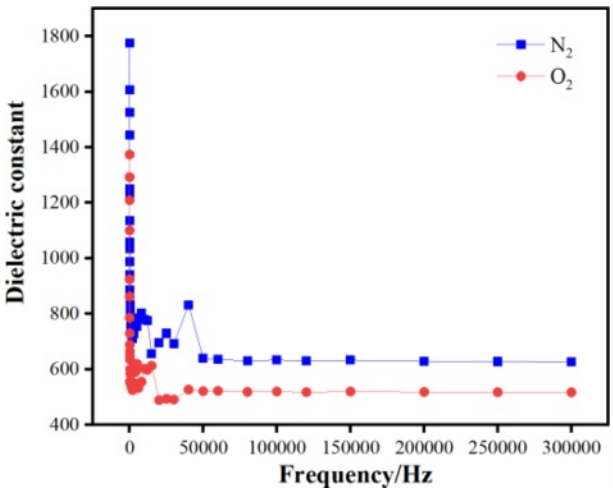

Fig. 5. Dielectric spectra of ceramic samples under different sintering atmospheres.

The stability of the dielectric constant in the high frequency band was determined by calculating the variance of the dielectric constant for frequencies greater than 50,000 Hz. The variance was 7.3 for sample 1 and 2.84 for sample 2, it can be seen that ceramics sintered in N_2 atmosphere are more stable in the high frequency stage. The dielectric loss is about 0.014 for sample 2 and 0.023 for sample 1 in the high frequency stage, so the dielectric loss of the BSIT ceramics sintered in N_2 atmosphere is reduced by about 39% in the high frequency stage compared to the O_2 sintering atmosphere.

Fig. 6 shows the variation of the dielectric loss of sample 1 and sample 2 between the test frequencies of 20 Hz and 300000 Hz. The dielectric constant decreases monotonically with frequency, and the dielectric loss tends to decrease first and then increase with increasing frequency, with an extreme value at a certain frequency. These properties are consistent with the frequency characteristics of the medium with relaxation polarization and cross-conductivity, indicating the presence of ion relaxation polarization and leakage currents in the BSIT

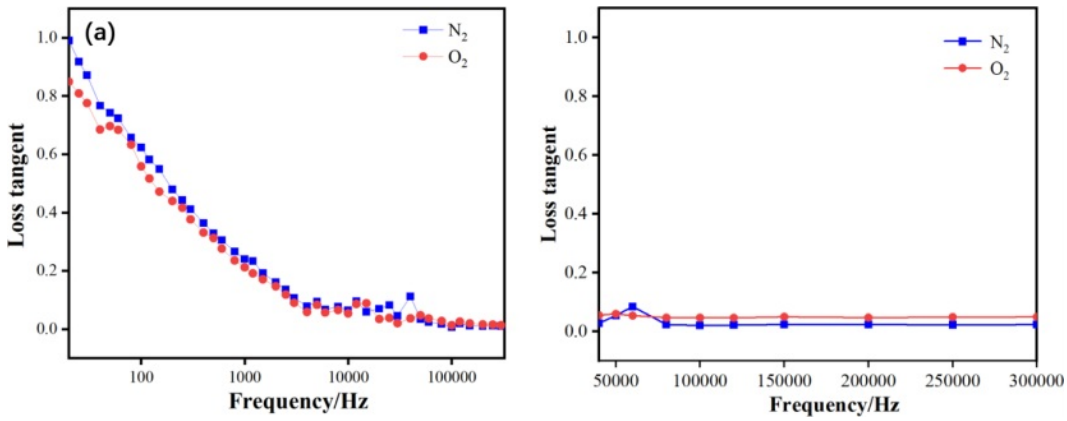

Fig. 6. Dielectric loss spectra of ceramic samples under different calcination atmospheres (a) Low frequency stage; (b) High frequency stage.

ceramic samples. This is due to the high concentration of crystal defects caused by the volatilization of Se^{2+} ions and the formation of oxygen vacancies at high temperatures, the concentration of relaxation ions is high, and the polarization mechanism is dominated by space charge polarization and ion relaxation polarization. When the frequency is higher, the space charge polarization and ion relaxation polarization are not established in time, the dielectric constant decreases and the loss increases. However, in the low frequency stage, the dielectric loss of sample 2 is higher than that of sample 1, probably because at low frequencies, the molecules and ions in the medium move relatively slowly and are more restricted by the lattice, so it is difficult for the medium molecules to deflect rapidly under the action of the electric field, resulting in the conversion of energy into heat, which results in a larger dielectric loss, and because the particle size of sample 2 is larger than that of sample 1, the molecules and ions move further and slower, so the dielectric loss of sample 2 is higher than that of sample 1. In the high frequency stage, the dielectric loss of sample 2 is lower than that of sample 1 because: as the frequency increases, sample 2, which has a denser surface, forms stable molecular and ion movement channels inside compared to sample 1, which has a higher surface porosity, and the concentration of oxygen vacancies is higher in the N_2 atmosphere, and the high temperature The volatilisation of Se^{2+} generates cation vacancies that complex with oxygen vacancies and weakly linked electrons are bound by the cation vacancies, leading to a reduction in leaky conductivity flow and smaller losses.

Summary

The BSIT ceramics obtained by sintering under N_2 and O_2 atmospheres were all of single chalcogenide structure, and the internal grain morphology was closely arranged round particles. The sintering atmosphere has a large effect on the densities and dielectric properties and dielectric losses of BSIT ceramics. The conclusions are as follows:

(1) In^{3+} doping has a greater influence on the microscopic morphology of BST ceramics, and the N_2 atmosphere allows In^{3+} to better enter the perovskite lattice, which is more conducive to promoting the grain growth and uniform distribution of ceramics, reducing microscopic defects and improving the densities.

(2) Compared with O_2 atmosphere, BSIT ceramics sintered in N_2 atmosphere have higher dielectric constant, lower dielectric loss, and better stability at high frequencies in the frequency range of 20 Hz-30,000 Hz.

Unlike the previous more complicated process conditions such as changing the dopant type, adding firing aid, and sintering temperature, it provides a low-cost and feasible solution for the preparation of low-loss dielectric ceramics by simply changing the sintering atmosphere. In the following research, the sintering process will be attempted using other gases (like Ar) to investigate how other sintering atmospheres will change the structure of the ceramics, in addition to combining the sintering atmosphere with other processes such as doping, adding sintering aids and changing the sintering temperature, and will be extended from a single chalcogenide ceramic material to other types of functional ceramic materials. In terms of characterisation, we will no longer limit ourselves to the dielectric properties of ceramics, but will also investigate their electrical insulation, ferroelectricity and magnetic properties in order to produce highly reliable ceramics that will meet the needs of future devices.

References

1. Y.S. Park and E. Kim, J. Ceram. Process. Res. 23[6] (2022) 919-925.
2. A. Imane, Z. Abdelouahad, N. Elbinna, E. Mohamed, and D. Mohamed, J. Ceram. Process. Res. 24[2] (2023) 222-229.
3. M.V. Romanov, I.E. Korsakov, and A.R. Kaul, Chem. Vap. Deposition. 10[6] (2010) 318-324.
4. K. Shin, H. Chang, H.K. Sun, and O.Y. Sang, J. Ceram. Process. Res. 18[6] (2017) 421-424.
5. H. Matsuo, Y. Kitanaka, Y. Noguchi, and M. Miyayama, J. Asian. Ceram. Soc. 3[4] (2015) 426-431.
6. E.A. Nenasheva, A.D. Kanareykin, and N.F. Kartenko, J. Electroceram. 13[1-3] (2004) 235-238.
7. Florent, S. Lavizzari, and L. Dipiazza, IEEE. Trans. Elec. Dev. 64[10] (2017) 4091-4098.
8. Z.T. Li, Y. Yuan, M.H. Yao, L. Cao, B. Tang, and S.R. Zhang, Ceram. Int. 45[17] (2019) 22015-22021.
9. L.H. Ou, W.Q. Wang, and W.W. Wang, J. Chin. Ceramic. Soc. 23[3] (2020) 39-44.
10. W.Q. Luo, Z.P. Li, and L.H. Yuan, Mod. Tech. Ceram. 43[1] (2022) 57-65.
11. R. Lin, D.Z. Xie, and Y. Hu, Chin. Ceram. 54[12] (2018) 42-46.
12. H. Jia and Y. He, J. Yang. Univ. 33[1] (2011) 20-23, 279.
13. W. Liu, H.X. Sun, J.H. Wang, and Y.G. Dong, J. Chin. Ceram. Soc. 50[3] (2022) 691-697.
14. Q. Yuan, G.B. Liu, and S. Wang, Chin. J. Inorg. Chem. 39[3] (2023) 485-491.
15. J. Lina, B. Wang, and H.G. Zhang, J. Chin. Ceram. Soc. 55[7] (2019) 42-47.
16. X. Jing, H.X. Liu, B. He, and Y.Q. Liao, J. Ceram. Process. Res. 11[3] (2010) 354-357.
17. M.L. Li, P.Y. Du, and S. Ji, Ordan. Mater. Sci. 32[6] (2009) 1-4.
18. B. Duan, Y. Luo, and B. Xu, Inf. Rec. Mater. 22[5] (2021) 1-5.
19. F.Q. Zhang, C.Z. Li, H.W. Li, and X.D. Guo, J. Ceram. Process. Res. 19[2] (2018) 101-104.
20. M. Michálková, M. Michálek, G. Blugan, and J. Kuebler, Adv. Appl. Ceram. 117[8] (2018)485-492.
21. H.C. Thong, Q. Li, M.H. Zhang, C.L. Zhao, K.X. Huang, J.F. Li, and K. Wang, J. Am. Ceram. Soc. 101[8] (3393-3401).